Fresnel Diffraction from Phase Steps and Its Applications

Mohammad Taghi Tavassoly[a] and Hamid Salvdari[b]

[a]Department of Physics, College of Science, University of Tehran, Tehran, Iran
[b]Department of Physics, Ilam Branch, Islamic Azad University, Ilam, Iran

***Corresponding author Email: tavassoly@ut.ac.ir**

Regular paper: Received: Nov. 8, 2020, Revised: Feb. 21, 2021, Accepted: Feb. 23, 2021, Available Online: Feb. 25, 2021, DOI: 10.29252/ijop.14.2.195

ABSTRACT— The well-established Fresnel diffraction occurs as an opaque object partially obstructs the passage of a coherent beam of light. In this process, the amplitude of the optical wave experiences a discontinuous change that leads to peculiar bright and dark fringes near the ray optics border of the beam. The fringe pattern varies very slowly by distance from the object and away from the beam border the diffraction effect is negligible. These behaviors have limited the applications of the conventional Fresnel diffraction very severely. In this article, we introduce a new kind of Fresnel diffraction that occurs due to discontinuous change in phase or phase gradient, in a part of a coherent beam of light. The change splits the beam into two diffracting wavefronts with common border that interfere with each other. In this kind of diffraction, the fringes may appear in the central part of the beam and their locations and visibilities are very sensitive to the phase change. Therefore, the researchers have utilized the effect in the measurements of different physical quantities, with high accuracy, using modest equipment. In this article, we use the Fresnel diffraction from the semi-infinite opaque screen (knife- edge) as the building block to describe the introduced effect, diffraction from the phase steps, and discuss its different aspects. We simulate the implied diffraction patterns, investigate the patterns by experiments, elaborate on the unique features of the effect, and present some interesting applications.

KEYWORDS: Fresnel diffraction, phase step, physical optics, metrology,

I. INTRODUCTION

Fresnel diffraction is a fundamental topic in physical optics. The well-established Fresnel diffraction appears as peculiar fringes on a plane perpendicular to the direction of a light beam, in the neighborhood of the ray optics boundary. In textbooks, the authors describe the effect by applying Fresnel–Kirchhoff integrals [1,2]. A well-treated example is the diffraction of a parallel beam of light from a straightedge [knife-edge], Fig. 1(a), which leads to the diffraction pattern shown in Fig. 1(b), with the intensity profile presented in Fig. 1(c). By applying Fresnel-Kirchhoff integrals, we calculate the complex amplitudes of the light at points P and P' in Fig. 2(a), located in the ray optics bright and shadow parts, respectively [3]:

$$U_P = \frac{-iA}{\lambda}\int_{-\infty}^{+\infty} dy \int_0^{+\infty} \tfrac{1}{r} e^{ikr} dx \qquad (1)$$

In Fresnel approximation, $r \cong R$ in the denominator and $r \cong R + \left[\left(x - x_P\right)^2 + \left(y - y_P\right)^2\right] \Big/ 2R$ in the exponential, this leads to

$$U_P\left(x_1\right) = \frac{A(1-i)}{2}\left[\left(\frac{1}{2} + C_1\right) + i\left(\frac{1}{2} + S_1\right)\right] \qquad (2)$$

and

[Downloaded from ijop.ir on 2026-01-29]

$$U_{P'}(x_2)=\frac{A(1-i)}{2}\left[\left(\frac{1}{2}-C_2\right)+i\left(\frac{1}{2}-S_2\right)\right] \quad (3)$$

where, A is the amplitude of the incident wave and

$$C_j+iS_j=\int_0^{V_j} e^{\frac{i\pi v^2}{2}}dv\,,\ j=1,2 \quad (4)$$

are Fresnel integrals, with

$$V_j=\sqrt{\frac{2}{\lambda R}}x_j \quad (5)$$

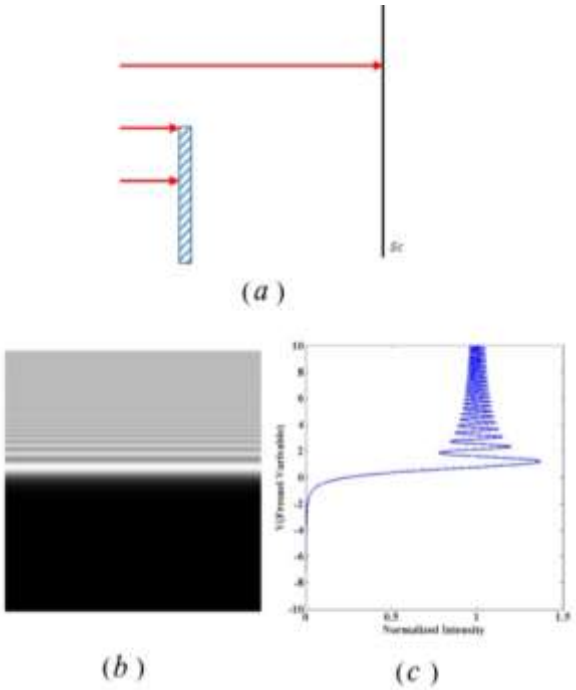

Fig. **1.** (*a*) A parallel beam illuminates a straight edge. (*b*) The simulation of the diffraction pattern of a straight edge (*c*) The associated normalized intensity profile versus the dimensionless Fresnel variable.

In Eq. (5), V_j, λ, and R stand for the dimensionless Fresnel variable, light wavelength, and the straightedge-observation plane distance, respectively. According to the Eqs. (2)-(5), the amplitudes of the interfering waves at points P and P' are determined by their distances from the borders of the beam. The plot of the normalized intensity versus Fresnel variable is a universal profile, Fig. 1(*c*). This profile permits one to determine the distance R in Eq. (5), by fitting the intensity profile versus x_j on the corresponding universal profile, for the given λ. In the Cornu spiral approach, a semi-infinite wavefront is associated to one-half Cornu spiral and $U_P(x_1)$ and $U_{P'}(x_2)$ in Eqs. (2) and (3) are the sum and the difference of the phasors **OJ** and **OP** in Fig. 2(*b*). As we will see, the semi-infinite wavefront is the building block for describing diffraction and interference in numerous cases.

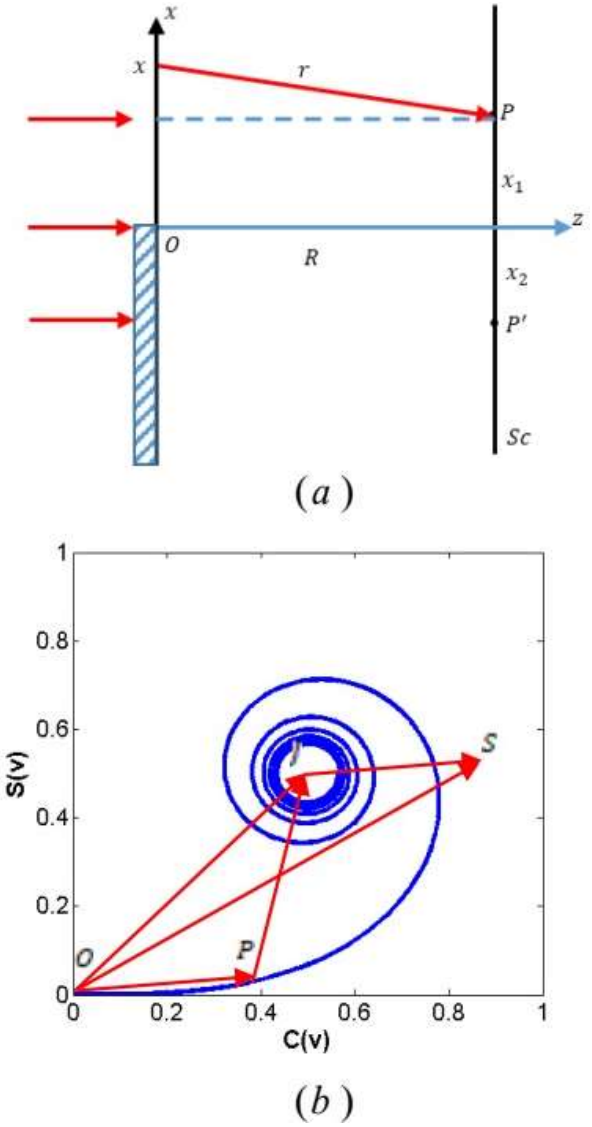

Fig. **2.** (*a*) The required geometry for calculation of the complex amplitude diffracted from a semi-infinite wavefront to point *P*. (*b*) One- half of the Cornu spiral can be used to determine the effective amplitude of a semi-infinite wavefront at an arbitrary point inside, **OS**, or outside, **PJ**, the ray optics bright area.

[Downloaded from ijop.ir on 2026-01-29]

In the interaction of light with transparent objects [phase objects], Fresnel diffraction can severely affect the intensity distributions associated with the neighborhood of the objects' borders. There are some rather old reports on the subject [4-9], but, systematic study of the effect, under the title "Fresnel diffraction from phase steps," has developed in the last two decades [3, 10-14]. This kind of the Fresnel diffraction occurs, as the phase or phase gradient, in a part of a coherent beam of light, undergoes a discontinuous change. In practice, discontinuous change in phase is realized as a beam of light reflects from a physical step, Fig. 3(*a*), or it passes through both sides of the edge of a transparent plate, Fig. 3(*b*).

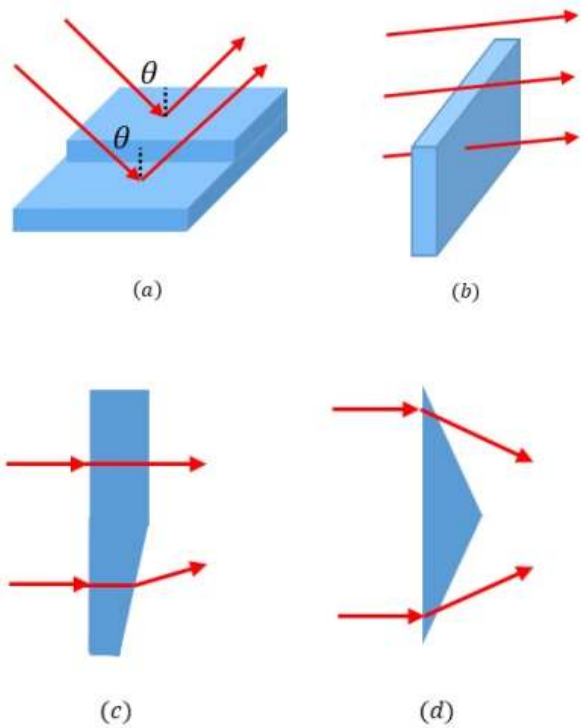

Fig. **3.** Discontinuous change in the phase of a beam occurs as the beam (*a*) reflects from a step, or (*b*) passes through the neighborhood of a transparent plate edge. Discontinuous change in the phase gradient occurs as a light beam (*c*) passes through a transparent plate with a wedge, or (*d*) passes through a bi-prism.

Discontinuous change in the phase gradient occurs, as a beam of light passes through a transparent plate with a wedge part, Fig. 3(*c*), or transmits through a Fresnel bi-prim, Fig. 3(*d*). The latter changes split the incident wave into two wavefronts with common border, (*a*) and (*b*), or into two intersecting wavefronts, (*c*) and (*d*), that interfere with each other. In this kind of interference, the diffraction effect can appear in the central part of the incident beam and can affect the intensity distribution severely. In fact, interference of two diffracted waves near the common border is involved that can be rigorously described by Fresnel-Kirchhoff integrals, and it covers the conventional diffraction and interference as the limiting cases [3]. We will show that this generalized interference or diffraction from a phase step has unique features compared with the conventional interference and diffraction, therefore, provides numerous interesting metrological applications that realize with high precision, using modest equipment.

II. Fresnel Diffraction from a Phase Step

When a parallel beam of light strikes a step of height h at angle of incidence θ, Fig. 3(*a*), the phase difference of the reflected wavefronts is [15]:

$$\varphi_0 = 2kh\cos\theta \tag{6}$$

where, k is the wavenumber. The phase difference for the wavefronts that transmit through and above a plane parallel plate, Fig. 3(*b*), is [15]:

$$\varphi_0 = 2kh\left(\sqrt{N^2 - N'^2\sin^2\theta} - N'\cos\theta\right) \tag{7}$$

where, h, N, and N' stand for the plate thickness, refractive index of the plate, and refractive index of the surrounding medium. The reflected or transmitted beams from the latter steps produce two non-overlapping parallel semi-infinite wavefronts with phase difference φ_0 . In Fig. 4(*a*) the traces of such wavefronts on the yz plane are represented by Σ_1 and Σ_2, with their common border along the y-axis. Using Eqs. (2) and (3), and considering Fig. 4(*a*), the diffracted amplitudes

[Downloaded from ijop.ir on 2026-01-29]

at point P inside the ray optics bright part of Σ_1 and outside the ray optics bright part of Σ_2, at distance x from the border plane, can be represented as:

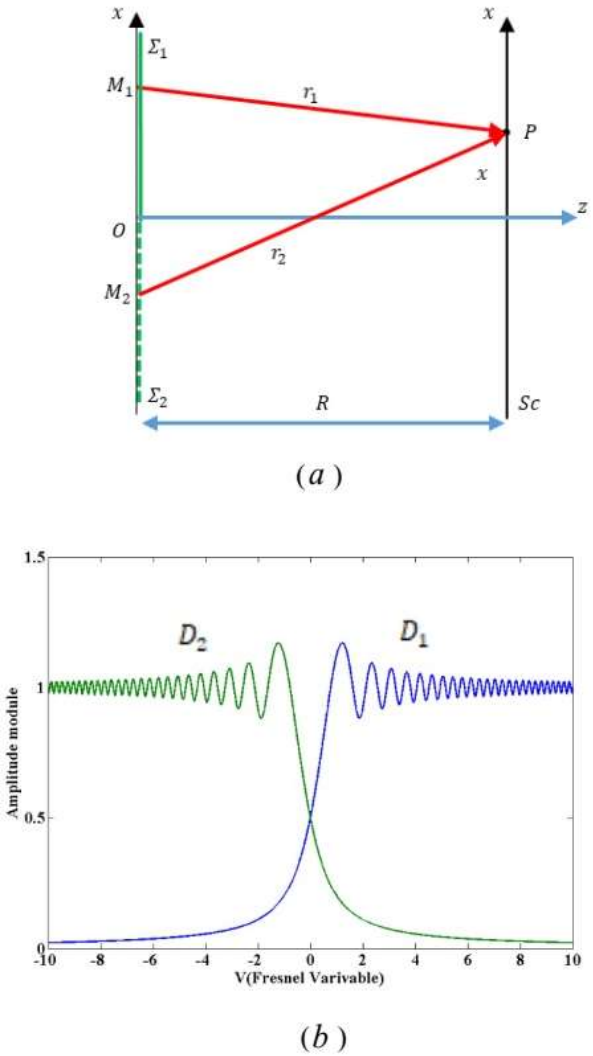

Fig. **4.** When a parallel beam of light reflects from or transmits through a step of constant height, it is splitted into two parallel plane wavefronts with a common border. (*a*) The traces of such wavefronts on the *xz* plane are represented by Σ_1 and Σ_2, with the common border along the *y* axis. (*b*) The moduli of the amplitudes of the diffracted wavefronts, D_1 and D_2, are plotted versus distance from the common border versus the Fresnel variable.

$$U_P(x)=\frac{A(1-i)}{2}\left\{\left[\left(\tfrac{1}{2}+C\right)+i\left(\tfrac{1}{2}+S\right)\right]+ te^{i\varphi_0}\left[\left(\tfrac{1}{2}-C\right)+i\left(\tfrac{1}{2}-S\right)\right]\right\} \quad (8)$$

where φ_0 is given by Eq. (5) or Eq. (6) and t is the ratio of the amplitudes reflected or transmitted from the two sides of the step edge. In a thin layer containing the ray optics border plane, practically, we have $C\cong S\cong 0$, and Eq. (8) reduces to

$$U_P=\frac{A}{2}\left(1+te^{i\varphi_0}\right) \quad (9)$$

which represents the interference of two ordinary waves with amplitudes $A/2$ and $tA/2$. Thus, intensity changes as a harmonic function, between $A^2(1-t)^2/4$ and $A^2(1+t)^2/4$, on the ray optics border plane. In the regions far away from the border plane, that is, where, $|V_j|>20$ [Eq. (5)], we have, practically, $|C|=|S|\cong 0.5$ and Eq. (8) reduces to A or $tAe^{i\varphi_0}$, which represent two non-interacting wavefronts with amplitudes A and tA, on two sides of the common border plane. In the regions corresponding to $0<|V_j|<20$, C and S vary rapidly with the distance from the border and interference is severely affected by diffraction. By representing the terms in the brackets of Eq. (8) by $D_1e^{i\delta_1}$ and $D_2e^{i\delta_2}$, the intensity at point $P(x)$ is represented by:

$$I_P(x)=\frac{A^2}{2}\left[D_1^2+t^2D_2^2+2tD_1D_2\cos(\varphi_0+\delta_2-\delta_1)\right] \quad (10)$$

Eq. (10) resembles the intensity equation in conventional interference. But, here D_1, D_2, δ_1, and δ_2 vary rapidly with distance from the common border plane and intensity at each point depends on phase φ_0 and the associated Fresnel variable. We should emphasize that in the introduced interference, contrary to the conventional interference, a fringe is not associated with a constant φ_0. In Fig. 4(*b*), the moduli of D_1 and D_2 are plotted versus the Fresnel variable. The plots indicate that the interference aspect of the diffracted waves is

[Downloaded from ijop.ir on 2026-01-29]

appreciable in the neighborhood of the common border plane. For $t \cong 1$, Eq. (10) reduces to [16]:

$$I_P = I_0\left[\cos^2\left(\frac{\varphi_0}{2}\right) + 2(C^2+S^2)\sin^2\left(\frac{\varphi_0}{2}\right) + (C-S)\sin\varphi_0\right] \quad (11)$$

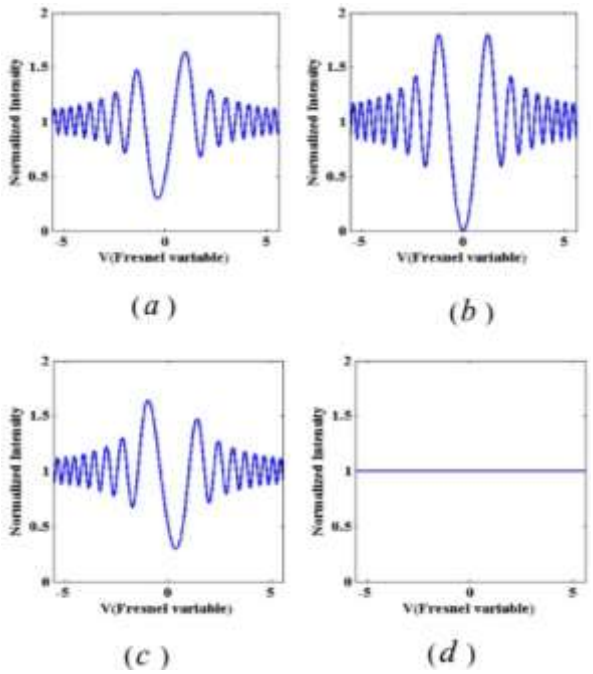

Fig. **5.** The normalized intensity profiles of the fringes of the light diffracted from a step with parallel surfaces versus the Fresnel variable for $\varphi_0 =$ (*a*) $\left(m+\frac{1}{2}\right)\pi$, (*b*) $(m+1)\pi$, (*c*) $\left(m+\frac{3}{2}\right)\pi$, and (*d*) $(m+2)\pi$, where *m* is an even number.

where $I_0 = A^2$. The plot of I_P / I_0 versus the Fresnel variable V is a universal curve for φ_0 in the interval of $0-2\pi$. This allows us to specify the experimental normalized intensity profiles accurately by fitting them on the corresponding universal curves. This is also applicable to the intensity equations with $t \neq 1$, if the universal curves for different, t and φ_0 are available. In Fig. 5, Eq. (11) versus V is plotted for $\varphi_0 = \left(m+\frac{1}{2}\right)\pi$, $(m+1)\pi$, $\left(m+\frac{3}{2}\right)\pi$, and $(m+2)\pi$, where *m* is an even number. Since the plots in Fig. 5 are universal for the given φ_0's, the normalized intensity equation, the visibility of the fringes, and distances of the intensity extremes from the border plane can be used to specify the associated phase. In Fig. 6(*a*), the visibility of the three central fringes [11]:

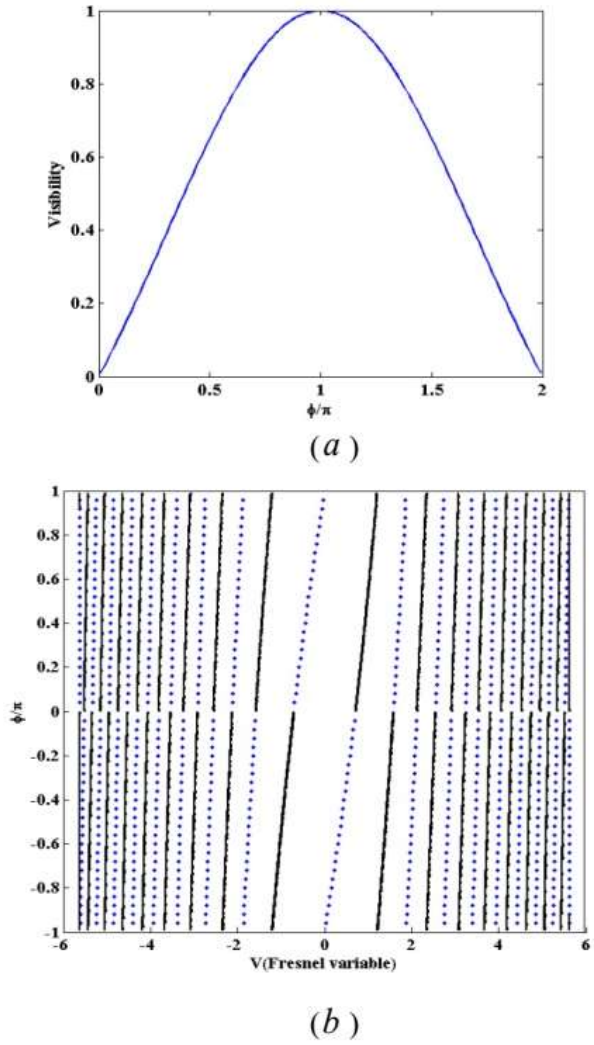

Fig. **6**. (*a*) The visibility of the three central diffraction fringes of a step with constant height versus the phase difference divided by π. (*b*) The plots of the locations of the intensity extremes of the step fringes versus the Fresnel variable for the phase change in the interval $-\pi < \varphi_0 < \pi$.

$$V = \frac{\frac{1}{2}\left(I_{LM} + I_{RM}\right) - I_{CM}}{\frac{1}{2}\left(I_{LM} + I_{RM}\right) + I_{CM}} \quad (12)$$

is plotted versus φ_0 / π. In Eq. (12), I_{LM}, I_{RM}, and I_{CM} represent the extreme intensities of the three central fringes. In Fig. 6(*b*), the distances of the intensity extremes, from the border plane, versus the Fresnel variable, are plotted for $-\pi < \varphi_0 < \pi$ [11]. We emphasize that the accurate specification of φ_0, which is

[Downloaded from ijop.ir on 2026-01-29]

possible by precision of $\pi/200$, allows us to measure the step height, the refractive index of the plate, and the wavelength of the incident light very accurately, provided one or two of the referred parameters are given [17-19].

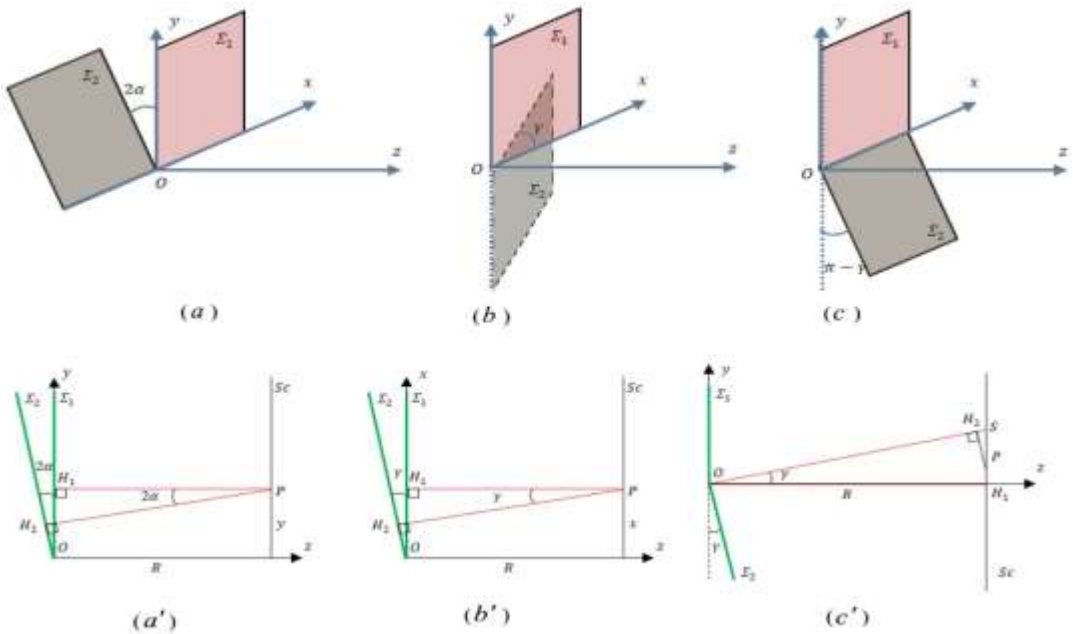

Fig. **7**. Illuminating the phase steps by a parallel beam of light the wavefronts Σ_1 and Σ_2 are produced. (*a*) The surfaces of the reflection step make angle α with each other. (*b*) The surfaces of the transmission step make angle α with the apex line perpendicular to the common border plane. (*c*) The surfaces of the transmission step make angle β with the apex line parallel to the common border. The described angles lead to the angles (*a*) 2α, (*b*) $\gamma=(n-1)\alpha$, and (*c*) $\gamma=(n-1)\beta$ between the corresponding wavefronts. The refractive index of the transmission steps is *n*. In Figs. (a'), (b') and (c'), the traces of the wavefronts on the page, are plotted that are used in calculation of phase difference.

So far, considering the diffraction effect, we studied the interference of two parallel wavefronts with common border plane that do not overlap in ray optics approach. Now, we extend the study, to the interference of two semi-infinite plane wavefronts with common border plane that make a small angle with each other. We express the amplitudes of the interfering wavefronts at each point, in terms of the distances of the point from the common border plane. The latter distances specify the required *C* 's and *S* 's. The phase difference of the wavefronts, φ, is determined by the distances of the point from the initial locations of the wavefronts. Thus, we express the amplitude of the interfering wavefronts as follows:

$$U_P(x,y)=\frac{A(1-i)}{2}\left\{\left[\left(\tfrac{1}{2}+C_1\right)+i\left(\tfrac{1}{2}+S_1\right)\right]+e^{i\varphi}\left[\left(\tfrac{1}{2}+C_2\right)+i\left(\tfrac{1}{2}+S_2\right)\right]\right\} \quad (13)$$

In Eq. (13), C_j and S_j, $j=1,2$ are positive for observation points locating in the bright part and negative for points locating in the shadow part of the wavefronts. The latter wavefronts appear, in reflection, when the surfaces of the step make a small angle α, with the apex line perpendicular to the common border plane. For a transmission phase step, this occurs when the surfaces of the plate make an angle α with the apex line perpendicular to the common border plane, or make a small angle β with the apex line parallel to the border plane. The wavefronts corresponding to these steps, Σ_1 and Σ_2, are illustrated in Figs. 7(*a*)-(*c*). The traces of the wavefronts, are

[Downloaded from ijop.ir on 2026-01-29]

plotted in Fig. 7(a')-(c'), to be used in calculations of the required amplitudes and phase changes. In the reflection step, Fig. 7(a), the wavefront Σ_1 extends along the positive x direction while wavefront Σ_2 continues along the negative x direction. The amplitude at point $P(x,y)$ with positive x, that depends on the distance from the border plane yz, is positive for Σ_1 and negative for Σ_2. The phase difference of the wavefronts at point P is determined by calculating $k(PH_2 - R)$ in Fig. 7(a'). Substituting the involved parameters in Eq. (13), leads to:

$$U_P(x) = \frac{A(1-i)}{2}\left\{\left[\left(\tfrac{1}{2}+C\right)+i\left(\tfrac{1}{2}+S\right)\right] + e^{i\varphi}\left[\left(\tfrac{1}{2}-C\right)+i\left(\tfrac{1}{2}-S\right)\right]\right\} \quad (14)$$

where,

$$V = \sqrt{\frac{2}{\lambda R}}x \quad (15)$$

and

$$\begin{cases}\varphi = \varphi_0 + ky\sin(2\alpha)\\ \varphi_0 = \varphi_{0x} - kR\left[1-\cos(2\alpha)\right]\end{cases} \quad (16)$$

In Eq. (16), φ_{0x} is the phase difference along x axis. It depends on the step height at the origin of the coordinate system. Considering Eq. (14) and φ in Eq. (16), we see that the intensity distribution along y axis is periodic, and diffraction effect is appreciable near yz plane, the common border. Far away from the yz plane, on both sides, we have, practically, no interference. The wavefronts in Fig. 7(b') are similar to the wavefronts in Fig. 7(a') and can be described by Eqs. (14)-(16) provided 2α is replaced by $\gamma = (n-1)\alpha$ and x by y, where, n is the refractive index of the plate. The wavefronts in Fig. 7(c') make an angle $(\pi - \gamma)$ with each other where, $\gamma = (n-1)\beta$. In this case, the wavefronts overlaps in the region bounded by SOH_1 and the corresponding C_1 and C_2 in Eq. (13) are positive. Thus, we can represent the interference at point $P(x,y)$ as follows:

$$U_P(x,y) = \frac{A(1-i)}{2}\left\{\left[\left(\tfrac{1}{2}+C_1\right)+i\left(\tfrac{1}{2}+S_1\right)\right] + e^{i\varphi}\left[\left(\tfrac{1}{2}+C_2\right)+i\left(\tfrac{1}{2}+S_2\right)\right]\right\} \quad (17)$$

where,

$$V_1 = \sqrt{\frac{2}{\lambda R}}y \quad (18)$$

$$V_2 = \frac{2\left(R\sin\gamma - y\cos\gamma\right)}{\sqrt{2\lambda\left(R\cos\gamma - y\sin\gamma\right)}} \quad (19)$$

and

$$\varphi = \varphi_0 + kR\left(1-\cos\gamma\right) - ky\sin\gamma \quad (20)$$

When β is small, Eqs. (19) and (20) reduce to

$$V_2 = \sqrt{\frac{2}{\lambda R}}\left[R(n-1)\beta - y\right] \quad (21)$$

and

$$\varphi = \varphi_0 - ky\left[(n-1)\beta\right] \quad (22)$$

Derivation of the amplitudes and phase difference for wavefronts emerging from a phase step with arbitrary orientation of its surfaces is rather complex [13, 16]. Therefore, we do not consider here, and conclude the section by presenting some relevant simulations. In Fig. 8, the simulations of the interference patterns of two wavefronts with common border, emerged from different phase steps, are shown: (a) parallel non-overlapping wavefronts with phase difference $\varphi = (2m+1)\pi$, (b) wavefronts in reflection that make an angle $2\alpha = 0.2°$, (c) wavefronts in transmission making an angle $\gamma = (n-1)\alpha$, $n = 1.5$, $\alpha = 0.2°$, and $\beta = 0$, (d) wavefronts

[Downloaded from ijop.ir on 2026-01-29]

in transmission making an angle $\gamma=(n-1)\beta$, $n=1.5$, $\alpha=0$, and $\beta=0.6°$, and (e) wavefronts with angles $\alpha=0.2°$, $\beta=0.6°$ and $n=1.5$. For these simulations, the distance between the step and the observation screen was $R=100mm$, and the observation screen was parallel to one of the wavefronts. These patterns clearly indicate that Fresnel diffraction from a phase step is very sensitive to the step height, refractive index, and angles between the step surfaces. Therefore, the subject is very rich and provides new techniques for measuring different physical quantities in small scales.

In this part of the article, we consider phase steps that diffract light by imposing discontinuous changes in the phase gradient. This kind of diffractions occur, for example, in Fresnel bi-prism, Fig. 9(a), and in a plate with a wedge part (PWP), Fig. 9(b). The latter elements split the incident beam into two intersecting wavefronts with common border [3, 14, 20]. In Fig. 9, the traces of the emerging wavefronts, Σ_1 and Σ_2, are shown. These wavefronts resemble the wavefronts shown in Fig. 7(c'). Therefore, we use Eq. (17) for describing the associated interference. For a bi-prism we have

$$V_1=\sqrt{\frac{2}{\lambda R}}\left(R\sin\gamma-y\cos\gamma\right)$$
$$V_2=\sqrt{\frac{2}{\lambda R}}\left(R\sin\gamma+y\cos\gamma\right) \qquad (23)$$

and

$$\varphi=\varphi_0-2ky\sin\gamma \qquad (24)$$

while, for a PWP we have:

$$V_1=-\sqrt{\frac{2}{\lambda R}}y$$
$$V_2=\sqrt{\frac{2}{\lambda R}}\left(R\sin\gamma+y\cos\gamma\right) \qquad (25)$$

and

$$\varphi=\varphi_0-2k\sin\left(\frac{\gamma}{2}\right)\left[R\sin\left(\frac{\gamma}{2}\right)+y\cos\left(\frac{\gamma}{2}\right)\right] \qquad (26)$$

In both cases, we have interference of two partially overlapped wavefronts. The overlapping regions are S_1OS_2 for the bi-prism and H_1OS for the PWP. In the case of the bi-prism, the phase difference does not change over the xz plane, while it changes for the PWP. Near the borders of the wavefronts, the diffraction effect is appreciable, and it decreases by the increase of R and γ, in the area away from the borders of the wavefronts [3].

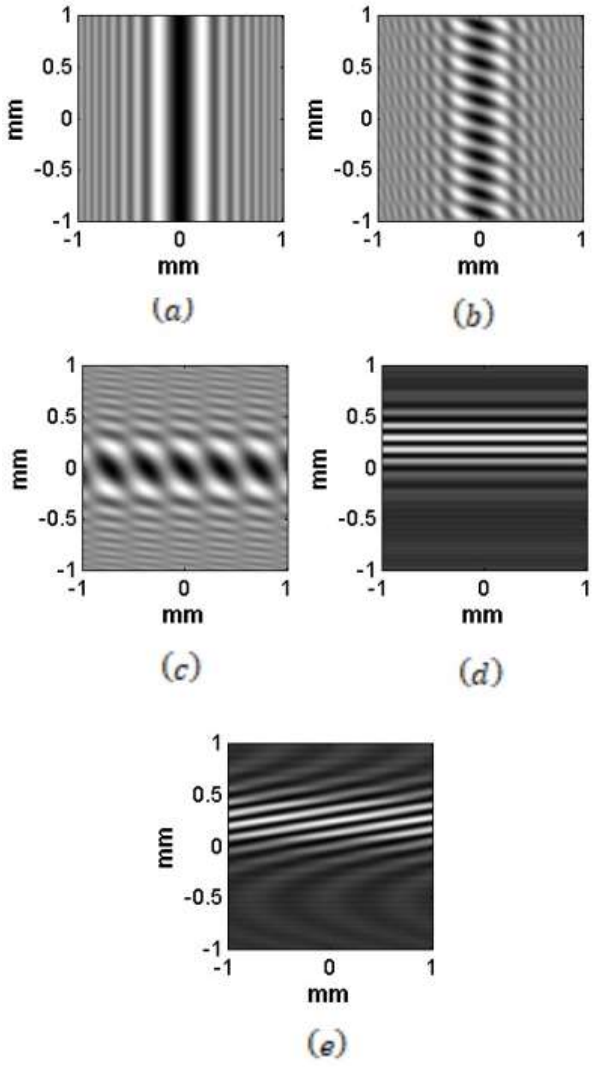

Fig. **8.** The simulated fringe patterns corresponding to the wavefronts represented in Fig. 7 for the angles, (a) $\alpha=0, \beta=0$ (b) $\alpha=0.1°, \beta=0$, (c) $\alpha=0.2°, \beta=0$, $n=1.5$, (d) $\alpha=0, \beta=0.6°$, $n=1.5$, and (e) $\alpha=0.2°, \beta=0.6°$, $n=1.5$.

[Downloaded from ijop.ir on 2026-01-29]

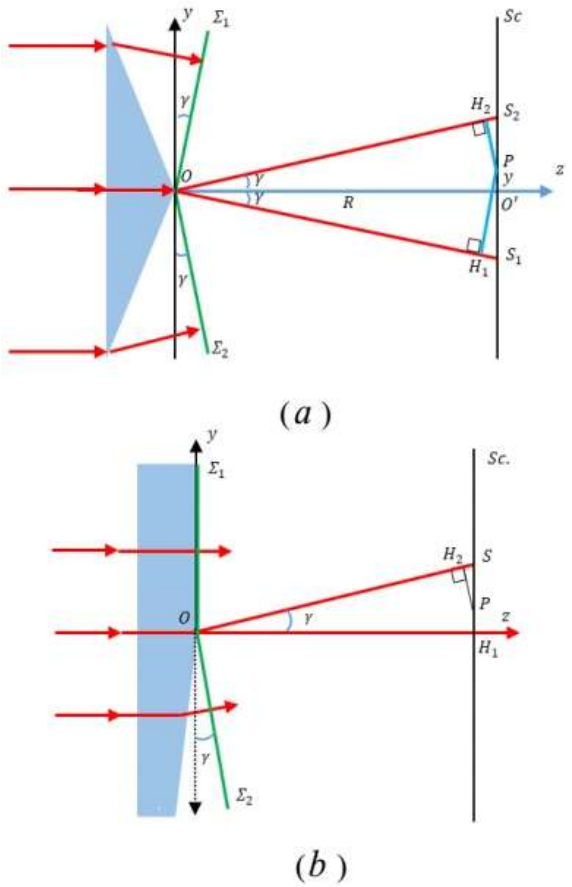

Fig. **9.** The side view of the wavefronts Σ_1 and Σ_2 emerging from (*a*) a bi-prism, (*b*) a transparent plate with a wedge part.

So far, using semi-infinite wavefronts, we discussed the interference of two diffracting wavefronts with common border. The wavefront can be limited on both sides, like a wavefront emerging through a slit. In this case, we replace the term $(1+i)/2$, in the derived equations, by $(C+iS)$ that is determined by the distance of the observation point from the second border of the wavefront. We can extend the approach to a wavefront that is limited from four sides. In this case, the amplitude, at observation point, depends on four distances. The phase step, limited from four sides, rectangular phase step of small size, can have interesting applications in quantitative phase microscopy.

III. SOME EXPERIMENTAL EXAMPLES

We have obtained the experimental intensity patterns shown in Fig. 10, by illuminating different phase steps, by a parallel beam of He-Ne laser, and recording at distance of $100mm$ from the steps. (*a*) Corresponds to a step with parallel surfaces. (*b*) Belongs to a step with the surfaces making angle $\alpha = 0.2°$, with the apex line perpendicular to the common border plane. (*c*) Associates with a step that its surfaces make angle $\beta = 0.2°$, the apex line parallel to the common border plane. (*d*) Corresponds to a step with the surfaces that make angles $\alpha = 0.1°$ and $\beta = 0.4°$ with each other. The experimental patterns, in Fig. 10, are in excellent agreement with the simulated patterns in Fig. 8.

IV. SOME INTERESTING APPLICATIONS

Before describing some applications, we prefer to elaborate on the unique features of the interference by phase steps.

Effective size of the step- According to the Cornu spiral for `1`1z, in practice, the diffraction effect is negligible. Considering Eq. (5), for $R = 100mm$ and $\lambda = 600nm$, we get $x \cong 3.4mm$ for $|V| = 20$, which implies that one can perform interferometry by a step of dimensions $6mm \times 10mm$, without requiring beam splitters and compensator plates.

There are only one or two closely located optical elements that are effective in producing fringes, therefore, mechanical noise is, practically, absent. Since there is no optical element between the step and the detector, the reflection step can cover very large range of wavelengths, from X-ray to IR.

The intensity distribution, the visibility of the fringes, and the locations of the intensity extremum, for phase change in the range $-\pi < \varphi < \pi$, have a universal profiles. This provides very accurate and reliable measurement of phase change.

In a phase step, we change the phase by varying the incident angle of the beam, while, in an interferometer, it is done by displacing a mirror. The precision in the former is much higher.

[Downloaded from ijop.ir on 2026-01-29]

We can evaluate the total interference order for a given step, by measuring the changes of the phases for two or more angular intervals. Using the total interference order, we can determine the step height and light wavelength, more accurately.

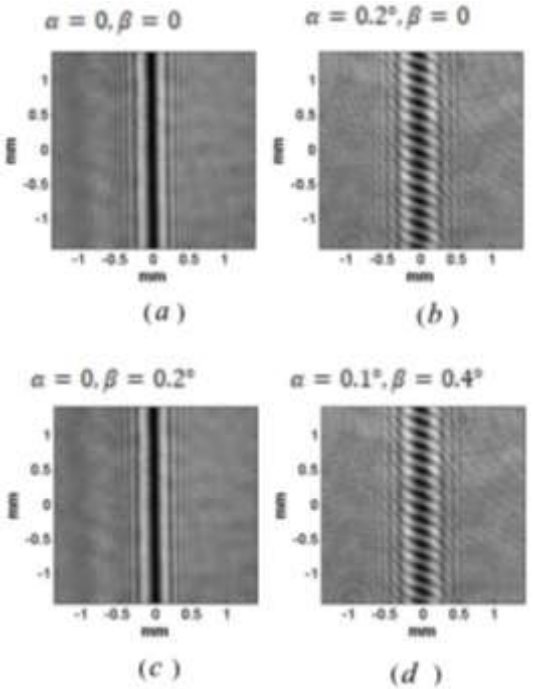

Fig. **10.** Experimental fringe patterns produced by steps with different angles, α and β, between their surfaces recorded at the distance 100 mm.

A. *Displacement sensor*

A flexible version of a reflection phase step is made of two rectangular mirrors A and B of several millimeters dimensions or more, mounted side by side on a stage, C in Fig. 11(*a*). One of the mirrors, A, can be displaced perpendicular to its surface, in order to change the step height. The other mirror, B, is equipped with the facility that allows to change its orientation. By mounting the mirror A, say, on a piezo electric element and illuminating the device as shown in Fig. 11(*a*), we get a high precision displacement sensor. Displacement of the mirror changes the visibility of the fringes, by recording the visibility of the three central fringes, we can detect the displacement by the precision of $\lambda/200$, comfortably [19]. The gadget is indispensable for the calibration of piezo electric devices.

Figure 11(*b*) illustrates the scheme of a transmission step interferometer. A parallel beam of light illuminates a transparent plate mounted on goniometer G. A detector mounted perpendicular to the transmission beam, records the diffraction fringes of the plate edge. As it has been shown in references [17, 18], by rotating the plate and recording the repetition of the visibility, one can measure the plate refractive index, plate thickness, light wavelength with high precision, provided one or two of the mentioned parameters are given [17, 18]. Installing the plate inside a cell containing a liquid, and rotating the cell, permits one to measure the refractive index of the liquid [18].

B. *Wavemetry*

For precise measurement of light wavelength, a reflection phase step with suitable height is required. Considering the coherence length of the given light, we choose a suitable step height approximately, by displacing the mirror A in Fig. 11(*a*). The more precise value of the step height is determined as follows. We mount the step on a goniometer and illuminate it by a parallel beam of light of large coherent length, with known wavelength. We mount the detector of the fringes on a rotatable arm perpendicular to the reflected beam. By rotating the phase step and counting the repetition of the visibility in angular interval, $(\theta_2 - \theta_1)$, precise height of the step is determined from Eq. (6). Since the phase change versus $\cos\theta$ is linear, by using several angles of incidence, the step height is determined by high accuracy. Repeating the experiment with the light of unknown wavelength, the wavelength is determined accurately. By selecting suitable step height one can determine the wavelength, coherence length, and spectral line profile of the given light easily. Applying this technique with modest equipment we have measured the wavelength with uncertainty of $\pm 0.01nm$ which can be improved readily [21].

[Downloaded from ijop.ir on 2026-01-29]

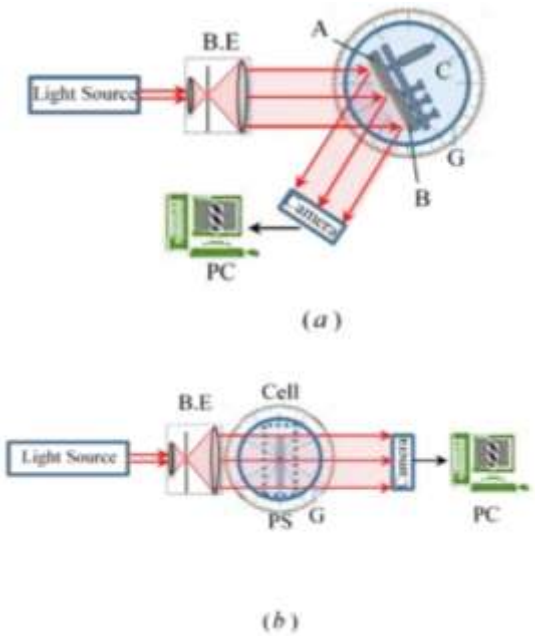

Fig. **11.** Two simple schemes of a phase step interferometer, (*a*) in reflection, (*b*) in transmission. As it is described in the text, they can be used to measure different quantities, including displacement, refractive index, and wavelength with high accuracy.

The second method for measuring an unknown wavelength is to use a transparent plate of constant thickness. We mount the plate at the center of a goniometer and illuminate its upper edge, by a parallel beam of the sample light. By rotating the plate in angular intervals $(\theta_2-\theta_1)$ and $(\theta_3-\theta_2)$ and recording the corresponding visibility repetitions, m_1 and m_2, Eq. (7) leads to

$$\frac{m_1+m_2}{m_1}=\frac{\left(\sqrt{N^2-\sin^2\theta_3}-\cos\theta_3\right)-\left(\sqrt{N^2-\sin^2\theta_1}-\cos\theta_1\right)}{\left(\sqrt{N^2-\sin^2\theta_2}-\cos\theta_2\right)-\left(\sqrt{N^2-\sin^2\theta_1}-\cos\theta_1\right)} \quad (27)$$

where, $N'=1$ is replaced for the refractive index of the surrounding medium. By solving Eq. (27), we obtain *N*. Considering Eq. (7), we can write:

$$m_1=\frac{2h}{\lambda}\left[\left(\sqrt{N^2-\sin^2\theta_2}-\cos\theta_2\right)-\left(\sqrt{N^2-\sin^2\theta_1}-\cos\theta_1\right)\right] \quad (28)$$

All the parameters in Eq. (28) are known except λ and *h*. By measuring *h*, we obtain λ. One can measure the thickness *h* by a micrometer or by applying Eq. (28) to a light source with known wavelength. Using this technique, we have measured wavelength with the precision of 0.1 nm [17].

C. *Measurement of refractive index*

Refractive index is an important physical parameter. Accurate measurement of refractive indices of small and thin plates is desirable. Fresnel diffraction from phase steps provides very simple and accurate methods for this kind of measurements. For example, the technique described in the second paragraph of section B, determines the refractive index of a plate without requiring thickness measurement. Applying this method, we have measured the refractive indices of plate samples by five significant figures [17]. Another method for measuring the refractive index of a transparent solid is to use a wedge shape sample with small angle between its surfaces. Illuminating the sample edge with a parallel beam, the fringes illustrated in Fig. 10(*b*) are formed. Using equation [15]

$$N=N'+\lambda/\rho\tan\alpha \quad (29)$$

where ρ is the fringe spacing at the edge surface, the refractive index is deduced. Immersing the wedge in a cell containing a liquid sample, leads to the determination of the liquid refractive index. Applying this technique, we have measured the refractive indices of solids and liquids by five significant figures [15].

D. *Measurement of diffusion coefficient*

We can apply Fresnel diffraction from a transmission step the measurement of diffusion coefficients in liquids, very easily and reliably [22]. Consider two liquids one on top of the other in a rectangular cell that are diffusing into each other, for example, water over sucrose solution. By installing a glass slide, vertically in the cell, Fig. 12(*a*), and

[Downloaded from ijop.ir on 2026-01-29]

illuminating the slide perpendicularly, by a monochromatic beam of light, we observe the diffraction pattern of the slide edge that its intensity distribution varies in time, because of the diffusion, Fig. 12(*b*). By evaluating the changes of the refractive index, at different times after the beginning of the diffusion, we can deduce the diffusion coefficient.

Finally, we should mention that the researchers have applied the Fresnel diffraction from a phase step to the measurements of the refractive index in X-ray region [23], film thickness [24-26], etching rate [27], simultaneous measurement of film thickness and refractive index [26], focal lengths of the lenses [28], specification of the spectral line profile [29], and modulation of phase function [30], Applications are increasing, particularly, in quantitative imaging of the phase objects in different scales [13, 31-32].

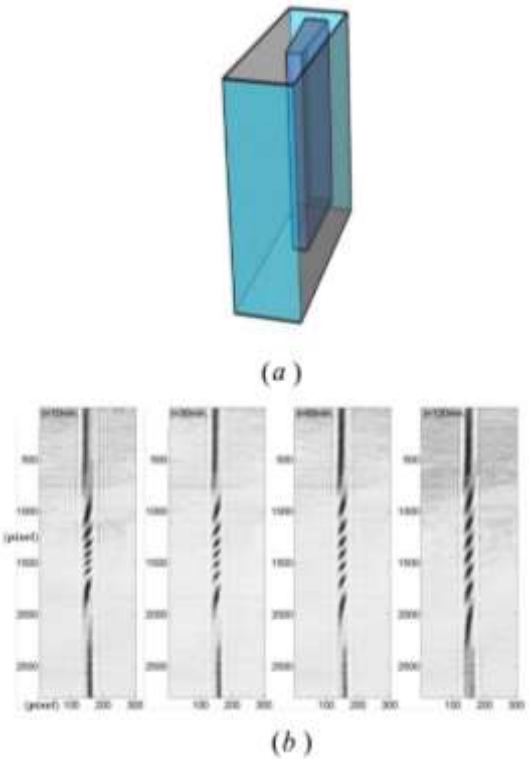

Fig. **12.** (*a*) A cell containing two liquids one on top of the other that diffuse in each other and a glass slide held vertically to produce the edge diffraction, (*b*) The diffraction patterns of the slide edge recorded 10, 30, 60, and 120 minutes after the beginning of the diffusion process.

V. CONCLUSION

This report shows that Fresnel diffraction from phase steps is a fundamental and rich subject with numerous interesting applications. It deals with the interference of diffracted modulated waves that produces a universal fringe pattern. The universal fringe pattern provides reliable and highly accurate measurement of the phase change.

The measuring techniques based on the interference of diffracted waves, compared with the corresponding techniques in conventional interferometry, are simpler, more precise, and less affected by mechanical noises. Besides, the former covers a very large range of wavelengths, from X-ray to far IR.

Fresnel diffraction from phase steps provides techniques for quantitative study of phase objects, which is very important in dealing with biomaterials.

The wavefronts produced in Fresnel diffraction from a phase step, are suitable object and reference waves for holographic study of small phase objects.

Finally, considering that diffraction occurs due to discontinuous change in amplitude and in phase of a wave, the authors should consider both effects, explicitly, in textbooks.

REFERENCES

[1] M. Born and E. Wolf, *Principles of Optics*, Cambridge University Press, Cambridge, England, 7nd Ed. 1999.

[2] E. Hecht, *Optics*, Pearson Education Incorporated, 5th Ed. 2017.

[3] M.T. Tavassoly and H. Salvdari, "Generalized interferometry," J. Opt. Soc. Am. A, vol. 35, pp. 2094-2103, 2018.

[4] C.V. Raman and I.R. Rao, "Diffraction of light by a transparent lamina," Proc. Phys. vol. 39, pp. 453–457, 1927.

[5] M.P. Givens and W.L. Goffe, "Application of the Cornu Spiral to the Semitransparent Half

[Downloaded from ijop.ir on 2026-01-29]

Plane," Am. J. Phys. vol. 34, pp. 248-253, 1966.

[6] H.D. Betz, "An Asymmetry Method for High Precision Alignment with Laser Light," Appl. Opt. vol. 8, pp. 1007-1013, 1969.

[7] O. Yoshihiro and M.C. Yin, "Fresnel diffraction by a semitransparent straight edge object with acoustically coherence-controllable illumination," Appl. Opt. vol. 23, pp. 300–306, 1984.

[8] L. Singher, J. Shamir, and A. Brunfeld, "Focused beam interaction with a phase step," Opt. Lett. vol. 16, pp. 61–63, 1991.

[9] M.H. Sussman, "Fresnel Diffraction with Phase Objects," Am. J. Phys. vol. 30, pp. 44-48, 1962.

[10] M. Amiri and M.T. Tavassoly, "Fresnel diffraction from 1D and 2D phase steps in reflection and transmission mode," Opt. Commun. vol. 272, pp. 349–361, 2007.

[11] M.T. Tavassoly, M. Amiri, A. Darudi, R. Aalipour, A. Saber, and A.R. Moradi, "Optical diffractometry," J. Opt. Soc. Am. A, vol. 26, pp. 540–547, 2009.

[12] E.V. Basisty and V.A. Komotskii, "Experimental investigation of laser beam diffraction on phase step and its practical applications," Electron. Lett. vol 50, pp. 693-695, 2014.

[13] H. Salvdari and M.T. Tavassoly, "Fresnel diffraction from the edge of a transparent plate in the general case," J. Opt. Soc. Am. A, vol. 35, pp. 496-503, 2018.

[14] E.A. Akhlaghi, A. Saber, and Z. Abbasi, "Fresnel diffraction due to phase gradient singularity," Opt. Lett. vol. 43, pp. 2840-2843, 2018.

[15] J.M.T. Tavassoly and A. Saber, "Optical refractometry based on Fresnel diffraction from a phase wedge," Opt. Lett. vol. 35, pp. 3679–3681, 2010.

[16] H. Salvdari, M.T. Tavassoly, and S.R. Hosseini, "Fresnel diffraction from a step in the general case," J. Opt. Soc. Am. A, vol. 34, pp. 674-680, 2017.

[17] M.T. Tavassoly, S.R. Hosseini, A.M. Fard, and R.R. Naraghi, "Applications of Fresnel diffraction from the edge of a transparent plate in transmission," Appl. Opt. vol. 51, pp. 7170–7175, 2012.

[18] J.M.T. Tavassoly, R.R. Naraghi, A. Nahal, and K. Hassani, "High precision refractometry based on Fresnel diffraction from phase plates," Opt. Lett. vol. 37, pp. 1493–1495, 2012.

[19] A.A. Khorshad, K. Hassani, and M.T. Tavassoly, "Nanometer displacement measurement using Fresnel diffraction," Appl. Opt. vol. 51, pp. 5066–5072, 2012.

[20] P. Torkaman, M. Amiri, and S.R. Hosseini, "Revisiting Young's edge diffracted wave: Diffraction of light by fractured plane wave-front," Optik, vol. 164, pp. 155-164, 2018.

[21] S.R. Hosseini and M. Tavassoly, "The application of a phase step diffractometer in wavemetry," J. Opt. vol. 17, No. 3, pp. 035605 (1-8), 2015.

[22] A. Saber and M.T. Tavassoly, "Measuring of diffusion coefficient of liquids using Fresnel diffraction from phase step," Proceedings of 21st Iranian Conference on Optics and Photonics, pp. 1053–1056, 2015.

[23] C.W. Gayer, D. Hemmers, C. Stelzmann, and G. Pretzler, "Direct measurement of the x-ray refractive index by Fresnel diffraction at a transparent edge," Opt. Lett. vol. 38, pp. 1563-1565, 2013.

[24] M.T. Tavassoly, I.M. Haghighi, and K. Hassani, "Application of Fresnel diffraction from a phase step to the measurement of film thickness," Appl. Opt. vol. 48, pp. 5497–5501, 2009.

[25] Kh. Hassani, M. Ashrafganjoie, and M.T. Tavassoly, "Application of white light Fresnel diffractometry to film thickness measurement," Appl. Opt. vol. 55, pp. 1803-1807, 2016.

[26] M. Jafari Siavashani, E.A. Akhlaghi, M.T. Tavassoly, and S. R. Hosseini, "Characterization of transparent thin films by low-coherent diffractometry," J. Opt. vol. 20, No. 3, pp. 035601 (1-6), 2018.

[27] A. Mahmoudi, "Application of Fresnel diffraction from phase steps to measurement of etching rate of transparent materials," Appl. Opt. vol. 54, pp. 7993-7996, 2015.

[Downloaded from ijop.ir on 2026-01-29]

[28] M. Dashtdar and S.M. Hosseini-Saber, "Focal length measurement based on Fresnel diffraction from a phase plate," Appl. Opt. vol. 55, pp. 7434-7437, 2016.

[29] A. Jabbari, Kh. Hassani, and M.T. Tavassoly, "Determination of the spectral line profile using a phase gradient step and stationary Fourier transform spectroscopy," Appl. Opt. vol. 58, pp. 5353-5359, 2019.

[30] M. Amiri, M.T. Tavassoly, H. Dolatkhah, and Z. Alirezaei, "Tunable spectral shifts and spectral switches by controllable phase modulation," Opt. Express, vol. 18, pp. 25089-25101, 2010.

[31] S. Ebrahimi and M. Dashtdar, "Application of Fresnel diffraction from a transparent plate in microscopy of phase samples," ICOP & ICPET _ INPC. vol. 23, pp. 741–744, 2017.

[32] S. Ebrahimi and M. Dashtdar, "Quantitative phase imaging based on Fresnel diffraction from a phase plate," Appl. Phys. Lett. vol. 115, pp. 203702 (1-5), 2019.

Mohammad Taghi Tavassoly is retired Professor of physics at Physics Department of the University of Tehran. His research interest is physical optics and its applications.

Hamid Salvdari was born in Shahriar, Iran, in 1977. He received the B.Sc. degree from the Kharazmi University, Tehran, Iran, in 2002, the M.Sc. degree from Zanjan University, Zanjan, in 2004, and the Ph.D. degree from University of Tehran, Tehran, in 2018, all in Atomic and molecular Physics. He is currently Assistant Professor at Islamic Azad University, Ilam branch, Ilam, Iran. His current research interest is physical optics and its applications.

[Downloaded from ijop.ir on 2026-01-29]